ACS OMEGA

Open Access

http://pubs.acs.org/journal/acsodf

Article

Powerful Approach for New Drugs as Antibacterial Agents via Molecular Docking and In Vitro Studies of Some New Cyclic Imides and Quinazoline-2,5-diones

Dalal Nasser Binjawhar, Ola A. Abu Ali, Arwa Sultan Alqahtani, Eman Fayad,* Ahmed M. Abo-Bakr,* Antonous. M. Mekhael, and Fayza M. Sadek

Cite This: *ACS Omega* 2024, 9, 18566−18575

Read Online

ACCESS | Metrics & More | Article Recommendations | Supporting Information

ABSTRACT: We generated novel elven 1,2,3,6-tetrahydrophthalimides and tetrahydroquinazoline derivatives from 1,2,3,6-tetrahydrophthalic anhydride (**1**) in response to our interest in using the anhydrides to produce heterocyclic nitrogen compounds. The elemental and spectral analyses of the produced compounds validated the recommended configurations and **MOE 2014.09** (Molecular Operating Environment) computations were used to perform their in silico analysis. The synthesized compounds have been analyzed and put through various experiments, including in vitro and in silico methods to assess their biological activity against *Escherichia coli* Penicillin-Binding Protein 3 (**PBP3**) and *Staphylococcus aureus* Penicillin-Binding Protein 2 (**PBP2**), among these compounds showing promising data as antibacterial drugs.

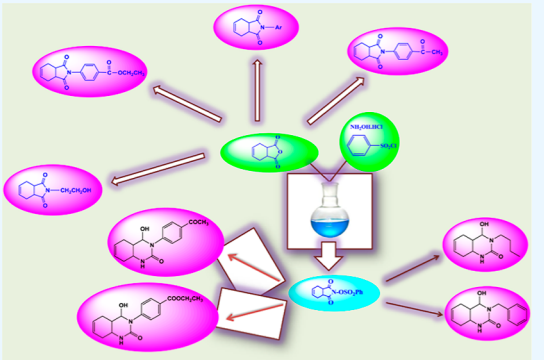

INTRODUCTION

Imide derivatives were reported as antibacterial, antifungal,[1] anticonvulsant activity,[2] liver function improvers, and therapeutic agents for liver disease.[3] Also, imide derivatives at 0.5 kg/ha preemergent gave slight (10−30%) control of weeds.[4] On the other hand, quinazoline derivatives cause vasodilation in animals,[5,6] and in vivo, testing showed that this in vitro activity translated to animal models predictive of chronic diseases such as depression and inflammation.[7,8] As well as, several advanced malignant bacterial forms have emerged because inappropriate antibiotic use in one patient can result in the establishment of a resistant strain that spreads to other people, each with varying levels of resistance to a therapeutic agent.[9,10] Our study mainly focused on PBP2a of *Staphylococcus aureus* (MRSA) that is fully resistant to all the ensuing generations of the β-lactam class of antibiotics, as exemplified by the penicillin structure. The primary basis for MRSA resistance to the β lactams is known.[11] The β-lactam antibiotics inactivate members of an essential family of enzymes, called penicillin-binding proteins (PBPs), which function in the biosynthesis of bacterial cell walls.[12] Moreover, PBP3 of *Escherichia coli* is an appealing therapeutic target for developing powerful inhibitors as antibacterial medication candidates. According to the Centers for Disease Control and Prevention, (CDC's) Antibiotic Resistance (AR) threats report, globally, 1.27 million people died, with around 5 million fatalities in 2019. So, to evade this resistance, we need to promise drugs. We had the objective of synthesizing new multiples (13 compounds) of 1,2,3,6-tetrahydrophthalimide and then assessing their efficacy as antibacterial agents against both Gram-positive and Gram-negative bacteria using in silico and in vitro methods.

RESULTS AND DISCUSSION

Chemistry. Treatment of anhydride **1** with different amines namely, benzylamine, *o*-aminothiophenol, *p*-aminoacetophenone, *p*-aminoethyl benzoate, and ethanolamine in addition to glycine in boiling acetic acid gave the corresponding imides **2**−**7** (Scheme 1).

There are two relatively stable conformers for cyclohexene carbocycle[13] in which the C_1-C_5 bond is quasiaxial (Figure 1A) in the structure corresponding to the inside form (relative to endo form) and quasiequatorial (Figure 1B) in the structure corresponding to the outside form (relative to exo form). In the determination of the preferred conformation of the *cis*-imides **2**−**7**, the inside conformer can be regarded as a homogeneous system in which the two carbonyl π-orbitals interact with the olefinic π-orbitals leading to a more stable conformer.

Received: February 5, 2024
Revised: March 19, 2024
Accepted: March 27, 2024
Published: April 10, 2024

Scheme 1. Reaction of the Anhydride 1 with Different Amino Compounds

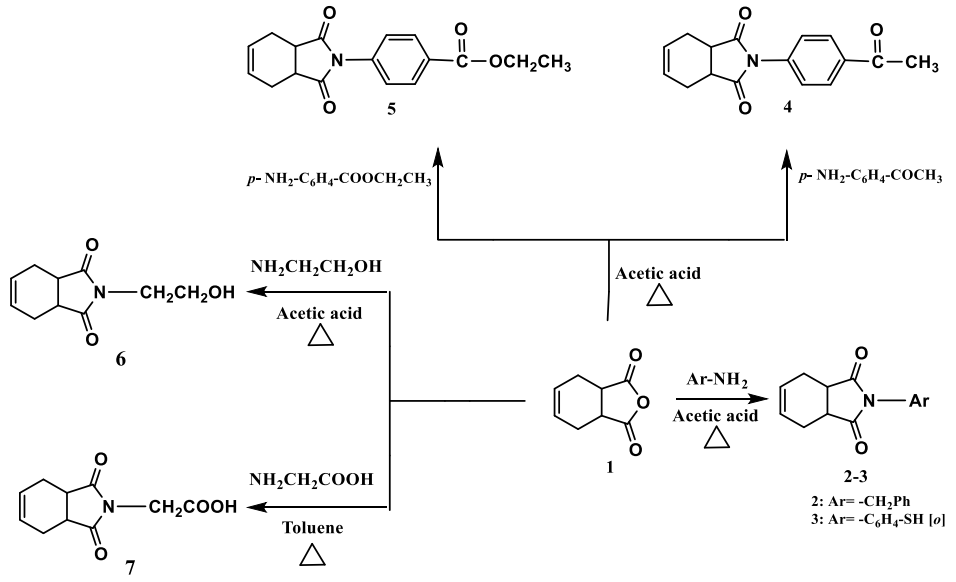

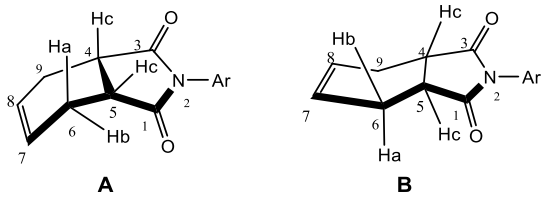

Figure 1. Quasiaxial and quasiequatorial conformers of the *cis*-imides **2**−**7**.

Formation of imide was proceed via nucleophilic attack of amino group of the aromatic amine (Ar-NH_2) on one carbonyl group of the anhydride **1** to yield corresponding amic acids at first, followed by intramolecular cyclization through the second ring closure by dehydration to produce the corresponding cyclic imide (Scheme 2).

Our motivation of our work is to synthesize new bioactive derivatives such as quinazolines. Thus, 2-phenylsulphonyloxy-3a,4,7,7a-tetrahydroisoindol-1,3-dione **8** was earlier prepared by Aly et al. and Abo-Bakr et al.[14,15] through the condensation of the anhydride **1** with hydroxyl amine hydrochloride in pyridine followed by replacement reaction with benzene sulphonyl chloride. So, when compound **8** was allowed to react with different aliphatic amines, namely, cyclohexylamine, butylamine, and different aromatic amines, namely, benzyl-amine, *p*-aminoacetophenone, *p*-aminoethylbenzoate in dry toluene or glacial acetic acid in the presence of sodium acetate, the corresponding tetrahydroquinazolinone **9**−**13** were obtained via Lossen rearrangement (Scheme 3), and the physical properties, elemental analysis, and spectral data of the synthesized compounds **2**−**13** were shown in (Tables 1 and 2).

It is worth mentioning that the spectral analyses of compounds **9**−**13** showed the presence of the sp3 proton of the C−OH group, as well as the disappearance of the two Hc protons of the hexene ring, providing clear evidence that these compounds prefer to remain more on the enol form than on the keto form (Table 2). This might be a result of the enol form's lower energy than the keto form.

The ^{1}H NMR data of the imides **2**−**7** (Table 2) showed the appearance of the two CH_2 protons in the carbocycle ring as identical protons for each of the two (CH_a and CH_b) and the appearance of the two H_c protons as multiplet as shown in (Figure 1). Whereas the ^{1}H NMR data of the quinazolinone **9**−**13** showed appearance of four identical protons of the two CH_2 groups in the carbocycle ring as a singlet, which affords evidence of the presence of planarity[16] of the cyclohexa-1,4-diene ring.

Scheme 2. Reaction Mechanism of the Anhydride 1 with Different Amines

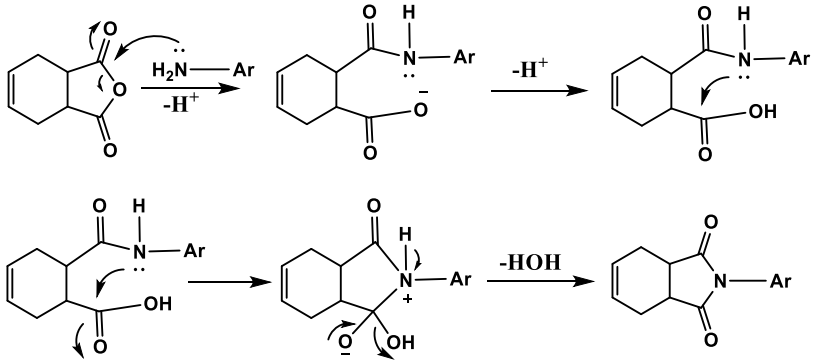

https://doi.org/10.1021/acsomega.4c01176
ACS Omega 2024, 9, 18566−18575

Scheme 3. Action of Different Amines on the *N*-Sulphonyloxy 8

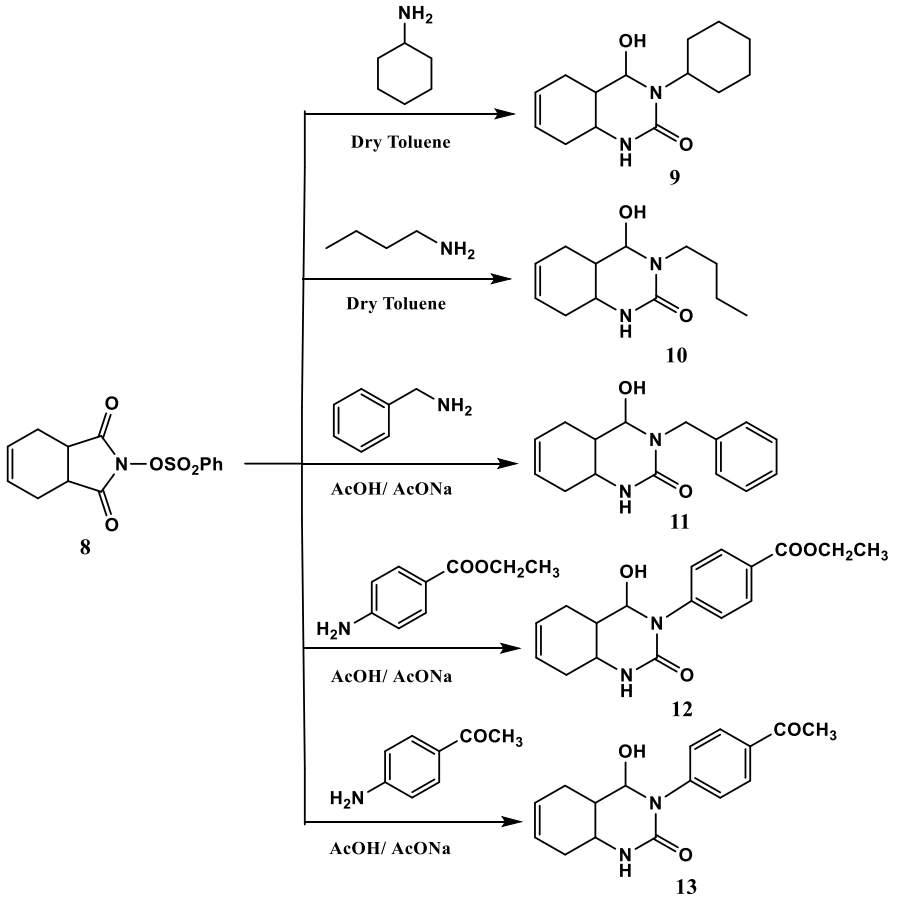

Table 1. Physical Data and Elemental Analyses of the Synthesized Compounds 2−13

comp.	Ar	mp °C	yield %	mol. formula (M. wt)	analysis				
						C %	H %	N %	S %
2	$-CH_2-Ph$	94−96	90	$C_{15}H_{15}NO_2$, 241.29	calc. found	74.67, 74.81	6.27, 6.06	5.80, 5.87	
3	$-C_6H_4SH$ (*o*)	198−200	95	$C_{14}H_{13}NO_2S$, 259.33	calc. found	64.84, 64.69	5.05, 5.18	5.40, 5.25	12.36, 12.54
4	$-C_6H_4COCH_3$ (*p*)	122−24	85	$C_{16}H_{15}NO_3$, 269.30	calc. found	71.36, 71.16	5.61, 5.31	5.20, 5.71	
5	$-C_6H_4COOC_2H_5$ (*p*)	150−52	90	$C_{17}H_{17}NO_4$, 299.33	calc. found	68.21, 67.98	5.72, 5.91	4.68, 4.74	
6	$-CH_2-CH_2-OH$	84−86	12	$C_{10}H_{13}NO_3$, 195.22	calc. found	61.53, 61.50	6.71, 6.66	7.17, 7.15	
7	$-CH_2-COOH$	104−06	98	$C_{10}H_{11}NO_4$, 209.20	calc. found	57.41, 57.17	5.30, 5.33	6.70, 6.91	
9	−cyclohexyl	170−72	27	$C_{14}H_{20}N_2O_2$, 248.33	calc. found	67.72, 67.58	8.12, 8.10	11.28, 11.29	
10	$-C_4H_9$	100−02	15	$C_{12}H_{18}N_2O_2$ 222.29	calc. found	64.84, 64.72	8.16, 8.20	12.60, 12.69	
11	$-CH_2C_6H_5$	154−56	18	$C_{15}H_{16}N_2O_2$, 256.31	calc. found	70.29, 70.23	6.29, 6.22	10.93, 10.90	
12	$-C_6H_4COOC_2H_5$ (*p*)	210−12	40	$C_{17}H_{18}N_2O_4$, 314.34	calc. found	64.96, 64.91	5.77, 5.78	8.91, 8.88	
13	$-C_6H_4COCH_3$ (*p*)	256−58	17	$C_{16}H_{16}N_2O_3$, 284.31	calc. found	67.59, 67.56	5.67, 5.60	9,85, 9.81	

DOCKING STUDY (IN SILICO)

Docking of the 13 Compounds into Penicillin-Binding Proteins (PBP2a and PBP3). The inhibitory effects observed can be attributed to the distinct structural differences in the cell walls of Gram-negative and Gram-positive bacteria. Gram-negative bacteria possess a cell wall composed of a thin peptidoglycan layer (7−8 nm) accompanied by an outer membrane. On the other hand, Gram-positive bacteria have a thick peptidoglycan layer (20−80 nm) outside the cell wall, lacking an outer membrane. Peptidoglycan, a mesh-like polymer consisting of sugars and amino acids, plays a crucial role in protecting microorganisms against antibacterial agents, including antibiotics, toxins, chemicals, and degradative enzymes.[17,18]

In this study, two different bacteria, *Staphylococcus* and *E. coli*, were chosen to explore potential antibacterial drug candidates using the MOE software technique. For each ligand molecule, multiple conformations were presented, and the best-fit conformation with a low binding energy and root mean square deviation (rmsd) was selected for further investigation.

PBP2a has a strong ability to distinguish and reject *β*-lactam antibiotics as potential inhibitors while showing a preference for the peptidoglycan substrate. This discrimination is facilitated by an allosteric site situated away from the active site. When this site is occupied correctly, it triggers the opening

https://doi.org/10.1021/acsomega.4c01176
ACS Omega 2024, 9, 18566−18575

Table 2. Spectral Data of Compounds 2−13

comp.	Ar	IR (cm^{-1})(KBr)	^{1}H NMR (ppm) ^{13}CNMR
2	$-CH_2-Ph$	(ν CH_2) 2950, 2900, 2850 (ν C=O's) 1715, 1680	(300 MHz/$CDCl_3$): 2.27 (m, 2H, $2CH_a$); 2.60 (m, 2H, $2CH_b$); 3.10 (m, 2H, $2CH_c$); 4.64 (s, 2H, CH_2) 5.89 (d, 2H, CH=CH); 7.28−7.31 (m, 4H, arom.)
3	$-C_6H_4SH$ (*o*)	(ν CH_2) 2950, 2900, 2850 (ν C=O's) 1710, 1680 (ν SH) 2550, 2500	(300 MHz/DMSO): 2.42 (m, 2H, 2 CH_a); 3.06 (m, 2H,$2CH_b$); 3.57 (m, 2H, $2CH_c$); 5.78 (t, 2H, CH=CH); 7.39−7.96 (m, 4H, arom.); 12.19 (s, 1H, SH)
4	$-C_6H_4COCH_3$ (*p*)	(ν CH-aromatic) 3250, 3150 (ν CH_2) 2950, 2850 (ν C=O's) 1700, 1690	(200 MHz/DMSO): 2.31 (m, 2H, $2CH_a$); 2.47 (m, 2H, $2CH_b$); 2.61 (s, 3H, CH_3); 3.35 (m, 2H, $2CH_c$); 5.96 (t, 2H, CH=CH); 7.93−8.07 (two dd., 4H, A2B2-system). ^{13}C NMR(100 MHz), DMSO-d_6, δ (ppm): 24.6 (CH_3), 27.4 ($2CH_2$−hexene), 41.7 (2CH−hexene), 124.3, 129.4, 136.6, 138.7 (Ar−C), 123.8 (CH=CH), 165.1, 171.4 (3C=O)
5	$-C_6H_4COOC_2H_5$ (*p*)	(ν CH-aromatic) 3250, 3150 (ν CH_2) 2950, 2900, 2850 (ν C=O's) 1710, 1680	(200 MHz/DMSO): 1.39 (t, 3H, CH_3); 2.30 (m, 2H, $2CH_a$); 2.74 (m, 2H, $2CH_b$); 3.28 (m, 2H, $2CH_c$); 4.40 (q, 2H, CH_2); 5.99 (t, 2H, CH=CH); 7.37−8.12 (two dd., 4H, A_2B_2-system)
6	$-CH_2-CH_2-OH$	(ν OH) 3600, 3200 (ν CH_2) 2950, 2900, 2850 (ν C=O's) 1710, 1680	(300 MHz/DMSO): 2.21−3.41(m, 10H, $2CH_a$, $2CH_b$, $2CH_c$, $2CH_2$); 4.7 (t, 1H, OH)); 5.88 (t, 2H, CH=CH)
7	$-CH_2-COOH$	(ν COOH) 3300, 2500 (ν CH_2) 2950, 2900, 2850 (ν C=O's) 1710, 1690	(300 MHz/DMSO): 2.25−2.89 (m, 6H, $2CH_a$, 2CHb, 2CHc); 4.05 (s, 2H, CH_2); 3.28 (m, 2H, $2CH_c$); 4.40 (q, 2H, CH_2); 5.86(t, 2H, CH=CH); 12.70 (s, 1H, COOH)
9	−cyclohexyl	(ν OH) 3400 (ν NH) 3275 (ν CH_2) 2950, 2900, 2850 (νC=O's) 1700, 1670	(300 MHz/$CDCl_3$): 1.23−2.89 (m, 14H, $7CH_2$); 3.74 (m, 1H, N−CH); 5.67−5.81 (dd, 2H, CH=CH); 6.78 (s, 1H, CH_{sp3}); 8.05 (s, 1H,OH); 8.51 (s, 1H, NH)
10	$-C_4H_9$	(ν OH) 3400 (ν NH) 3250 (ν CH_2) 3100, 3000 (ν C=O's) 1705, 1695	(300 MHz/DMSO): 0.97 (t, 3H, CH_3); 1.35−1.60 (m, 4H, $2CH_2$); 2.92 (s, 4H, $2CH_2$); 3.33 (t, 2H, NCH_2) 5.67−5.81 (dd, 2H, CH=CH); 6.79 (s, 1H, CH_{sp3}); 8.15 (s, 1H, OH); 8.60 (s, 1H, NH)
11	$-CH_2C_6H_5$	(ν OH) 3400 (ν NH) 3250 (ν CH-aromatic) 3100, 3000 (ν C=O)1705, 1695	(300 MHz/DMSO): 2.88 (s, 4H, $2CH_2$); 4.53 (2H, N−CH_2) 5.69−5.76 (dd, 2H, CH=CH); 6.83 (s, 1H, CH_{sp3}); 7.32(m, 5H, arom.); 8.68 (s, 1H, OH); 9 05 (s, 1H, NH). ^{13}C NMR(100 MHz), DMSO-d_6, δ (ppm): 18.2 (CH_2−hexene), 29.3 (CH_2−hexene), 41.5 (CH_2Ph) 46.1 (CH−hexene), 52.9 (CH−hexene), 91.5 (C−OH), 124.9 (CH=CH), 122.6, 127.7, 132.4, 137.8 (Ar−C), 152.9 (C=O)
12	$-C_6H_4COOC_2H_5$ (*p*)	(ν OH) 3400 (ν NH) 3300 (ν C=O) 1710, 1705 (ν CH-aromatic) 3100, 3000	(300 MHz/$CDCl_3$): 1.40 (t, 3H, CH_3) 3.01 (s, 4H, $2CH_2$); 3.73(q, 2H, OCH_2); 5.75−5.82 (two dd, 2H, CH=CH); 6.94 (s, 1H, CH_{sp3}); 7.63−8.03 (dd., 4H, arom. A_2B_2-system); 8.69 (s, 1H, OH); 11.04 (s, 1H, NH)
13	$-C_6H_4COCH_3$ (*p*)	(ν OH) 3400 (ν NH) 3250 (νC=O's) 1710, 1700	(300 MHz/DMSO): 2.37 (s, 3H, CH_3) 2.88 (s, 4H, $2CH_2$); 5.69−5.77 (dd, 2H, CH=CH); 6.91 (s, 1H, CH_{sp3}); 7.09−7.53 (m, 4H, arom.); 10.53 (s, 1H, OH); 10.99 (s, 1H, OH); 10.47 (s, 1H, NH). ^{13}C NMR (100 MHz), DMSO-d_6, δ (ppm): 25.2 (CH_3), 18.7 (CH_2−hexene), 28.3 (CH_2−hexene), 47.6 (CH−hexene), 51.1 (CH−hexene), 93.7 (C−OH), 123.8 (CH=CH), 119.5, 128.4, 136.9, 144.6 (Ar−C), 158.8, 166.7 (2C=O)

https://doi.org/10.1021/acsomega.4c01176
ACS Omega 2024, 9, 18566−18575

Table 3. Binding Energies of Synthesized Compounds 1−13 along with Positive Control and Their Interactions with the Allosteric Site of the Target Protein PBP2a

no	compounds	S kcal/mol[a]	rmsd_refine[b]	amino acid bond	distance Å
1	$C_8H_8O_3$	−5.46	1.7	Arg241/H-acceptor	3.34
2	$C_{15}H_{15}NO_2$	−6.75	2.4	Ser240/H-acceptor	3.11
3	$C_{14}H_{13}NO_2S$	−6.60	1.7	Thr165/H-donor	3.31
				Arg241/π−H	3.94
4	$C_{16}H_{15}NO_3$	−7.34	1.2	His293/H-acceptor	2.97
				His293/π−π	3.91
5	$C_{17}H_{17}NO_4$	−7.98	1.2	His293/H-acceptor	2.98
6	$C_{10}H_{13}NO_3$	−6.45	2	Arg241/H-acceptor	2.90
7	$C_{10}H_{11}NO_4$	−6.52	1.8	His293/H-acceptor	3.19
8	$C_{14}H_{13}NO_5S$	−7.62	1.6	Ser240/H-acceptor	3.29
9	$C_{14}H_{20}N_2O_2$	−6.80	1.5	Arg241/H-acceptor	2.85
10	$C_{12}H_{18}N_2O_2$	−6.72	2.4	Arg151/H-acceptor	2.97
11	$C_{15}H_{16}N_2O_2$	−6.97	0.8	Arg241/H-acceptor	2.85
12	$C_{17}H_{18}N_2O_4$	−8.30	1.3	Arg241/H-acceptor	3.32
				Arg241/H-acceptor	2.91
13	$C_{16}H_{16}N_2O_3$	−7.69	0.9	Arg241/H-acceptor	2.88
				Arg151/H-acceptor	2.95
				Arg241/π−H	4.36
	chloro-amphenicol (positive control)	−7.72	1.4	Thr216/H-donor	3.69
				Arg241/H-acceptor	3.09
				Ser240/H-acceptor	3.14
				Arg241/H-acceptor	3.24
				Arg151/H-acceptor	3.00

[a]Energy score. [b]Root mean square deviation.

of gatekeeper residues within the active site and alters the conformation of essential residues, allowing catalysis to occur.[19]

The docking of ligand molecules to *Staphylococcus* PBP2a showed a satisfactory fit to the allosteric site, as summarized in Table 3, with binding energies ranging from −5.46 to −8.30. The docking software visualized all docked ligands and recorded the most favorable poses along with the positive control in Figure 2.

Importantly, all compounds successfully bound to the target PBP2a receptor through hydrogen bond interactions and other types of interactions. Compound **1** exhibited a higher binding energy score (−5.46 kcal/mol) compared to those of the other compounds. The analogue labeled as **2** displayed a better binding energy (−6.75) to the target, forming a hydrogen bond acceptor interaction with Ser240 at 3.11 Å. Compound **3** was docked to the target's residues Thr165 and Arg241, forming hydrogen bond donor and π−H interactions, respectively. Compound **4** revealed a good binding energy (−7.34 kcal/mol) and engaged in two different interactions: a hydrogen bond acceptor interaction with His293 and a π−π interaction at distances of 2.97 and 3.91 Å, respectively. Furthermore, compound **5** had the second lowest binding energy (−7.98 kcal/mol) and interacted with residue His293 through a hydrogen bond at a distance of 2.98 Å. Compound **6** interacted with the target through a hydrogen bond acceptor interaction with Arg241 at a distance of 2.90 Å. Compound **7** showed interactions with the target residue His293 through a hydrogen bond at a distance of 3.19 Å. Compound **8** exhibited a good binding energy (−7.62 kcal/mol) and interacted with the target through a hydrogen bond with Ser240 at a distance of 3.29 Å. Similarly, compound **9** exhibited a good score and docked to the target's Arg241 residue through a hydrogen bond at a distance of 2.85 Å. Compound **10** (−6.72 kcal/mol) interacted with the target's residue Arg151 through a hydrogen bond at a distance of 3.04 Å. Compound **11** was docked to the target through a hydrogen bond at a distance of 2.85 Å. Successfully, Compound **12** (−8.30 kcal/mol) presented the lowest binding energy and acceptable RMSD when interacting with the target residue Arg241 through two different hydrogen bonds at distances of 3.32 and 2.91 Å. Compound **13** displayed a binding energy of −7.69 kcal/mol and a low RMSD, showing good interactions through hydrogen bond acceptor and π−H interactions with the residues Arg241, Arg151, and Arg241 at distances of 3.03 2.99, and 4.30 Å, respectively. Lastly, positive control exhibited the third-lowest binding energy (−7.72 kcal/mol) and demonstrated the highest number of five hydrogen bond interactions with the residues Arg241, Thr216, Ser240, and Arg151.

Regarding PBP3 (Table 4), the binding scores of the compounds with the target receptor PBP3 were slightly lower compared to those of PBP2a. Compound **1** exhibited a lower binding score (−4.71 kcal/mol) but showed an interaction with the target residue Lys152 through a hydrogen bond at 2.84 Å. However, compounds **2**−**13** showed better binding scores and acceptable rmsd values. Compound **2** interacted with the target residue Lys152 through a hydrogen bond (4.11 Å) and formed a π−H interaction with the same residue at 4.89 Å. On the other hand, despite the good binding score (−6.24 kcal/mol) and high hydrophobicity, compound **3** did not exhibit any hydrogen bond or π bond interactions. This was also true for compounds **6**, **9**, and **10**, with binding scores of −5.32, −5.92, and −6.24, respectively. Compounds **4** and **5** were docked to the target receptor and formed π−H bonds with Pro157 at distances of 3.71 and 3.63 Å, respectively. Compound **7** interacted with the target through three hydrogen bonds with residues Leu156, Ile159, and Ile151 at distances of 3.34 3.17, and 3.18 Å, respectively. Fortunately,

https://doi.org/10.1021/acsomega.4c01176
ACS Omega 2024, 9, 18566−18575

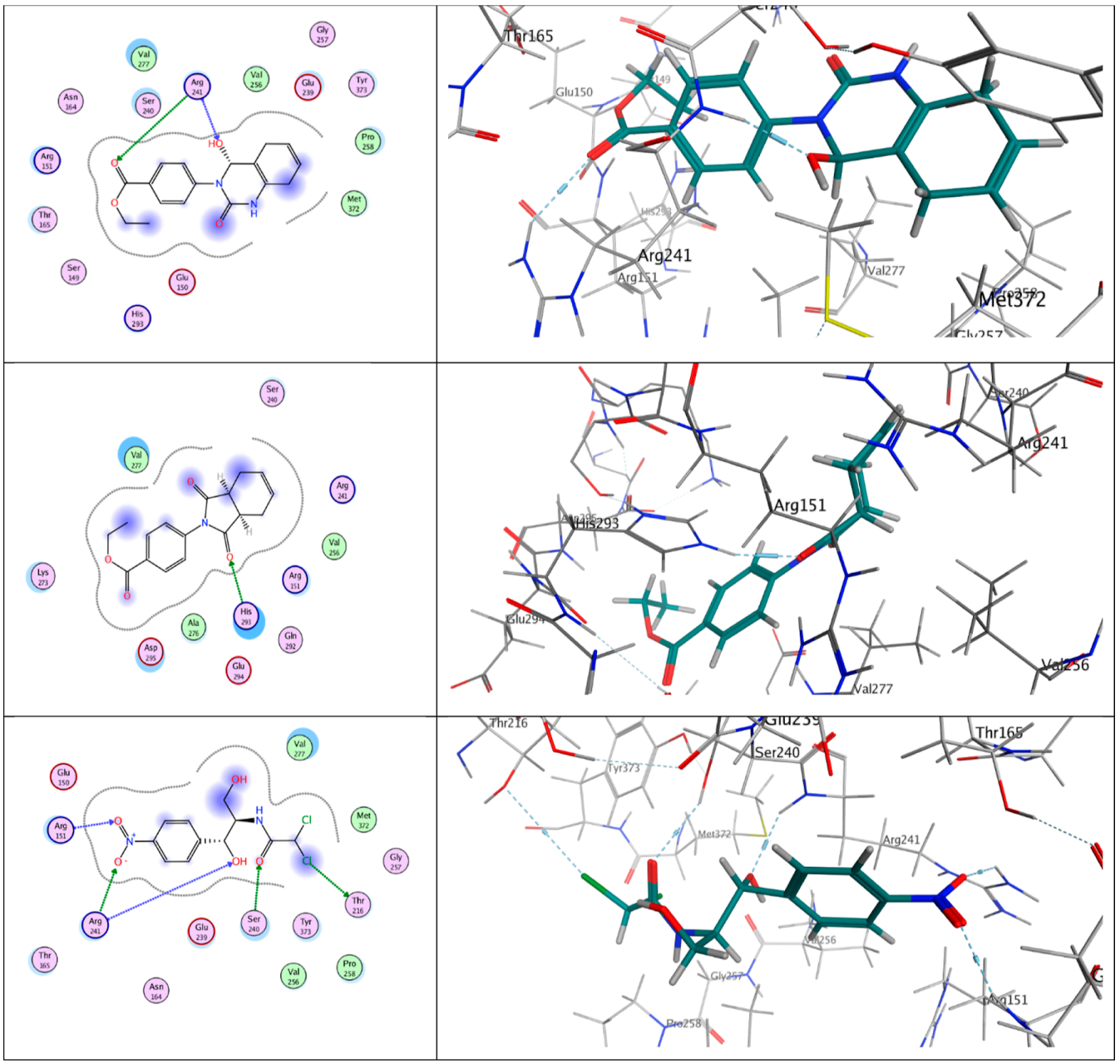

Figure 2. 2D (left side) and 3D (right side) docking orientations of the best-docked compounds **12**, **5**, and positive control with the allosteric site pocket of PBP2a.

compound **8** exhibited the third-best binding score (−7.26 kcal/mol) and docked to target residues Ile159 and His99 through hydrogen and H−π bonds. Compound **11** also had a low binding score (−7.18 kcal/mol) and interacted with the target residue Lys152 through π−cation and π−H bonds at distances of 4.97 and 3.71 Å. Compound **12** formed a hydrogen bond (2.96 Å) with the target residue Gly158 and another hydrogen bond (3.21 Å) with Glu97, with a low binding energy of (−7.16 kcal/mol). The second-best compound, labeled **13**, had a low binding score (−7.33 kcal/mol) and interacted with target residues Gly158 and Lys152 through hydrogen bonds. Lastly, positive control achieved the lowest binding score (−7.50 kcal/mol) among the 14 compounds, it docked to the target residue Lys152 through a hydrogen bond at 2.86 Å. The best docked 2 compounds and positive control are illustrated in (Figure 3).

Considering the various interaction modes observed during the theoretical study, it is hypothesized that the synthesized compounds serve a crucial function as antibacterial agents.

IN VITRO STUDY

Table 5 and Figures 4 and 5 present the outcomes of the sensitivity test conducted to assess the effectiveness of the synthesized compounds. This evaluation involved measuring the sizes of the inhibition zones formed by these compounds against *E. coli* and *S. aureus*.

According to the results, the recently synthesized compounds exhibited a positive effect in terms of inhibition zones. The effectiveness of the synthesized compounds in suppressing bacterial growth can be attributed to their interaction with peptidoglycans present in the cell wall. This suggests that these compounds possess promising biological properties.

https://doi.org/10.1021/acsomega.4c01176
ACS Omega 2024, 9, 18566−18575

Table 4. Binding Energies of Synthesized Compounds 1−13 along with Positive Control and Their Interactions with the Active Site of the Target Protein PBP3

no.	compound	S kcal/mol[a]	rmsd_refine[b]	amino acid bond	distance Å
1	$C_8H_8O_3$	−4.71	0.8	Lys152/H-acceptor	2.84
2	$C_{15}H_{15}NO_2$	−6.69	1.2	Lys152/π−H	3.67
				Lys152/π−cation	4.89
3	$C_{14}H_{13}NO_2S$	−6.24	1.6		
4	$C_{16}H_{15}NO_3$	−5.93	3.2	Pro157/π−H	3.62
5	$C_{17}H_{17}NO_4$	−6.50	3.2	Pro157/π−H	3.62
6	$C_{10}H_{13}NO_3$	−5.32	1.2		
7	$C_{10}H_{11}NO_4$	−5.41	1.9	Leu156/H-acceptor	3.34
				Ile159/H-donor	3.17
				Ile151/H-donor	3.18
8	$C_{14}H_{13}NO_5S$	−7.26	1.3	Ile159/H-donor	4.31
				His99/H−π	3.99
9	$C_{14}H_{20}N_2O_2$	−5.92	1.2		
10	$C_{12}H_{18}N_2O_2$	−6.24	1.2		
11	$C_{15}H_{16}N_2O_2$	−7.18	1.7	Lys152/π−cation	4.97
				Lys152/π−H	3.71
12	$C_{17}H_{18}N_2O_4$	−7.16	2.3	Gly158/H-acceptor	2.96
				Glu97/H-donor	3.21
13	$C_{16}H_{16}N_2O_3$	−7.33	1.1	Gly158/H-acceptor	2.90
				Lys152/H-acceptor	2.91
14	chloro-amphenicol (positive control)	−7.50	1.8	Lys152/H-acceptor	2.86

[a]Energy score. [b]Root mean square deviation.

ANTIBACTERIAL ACTIVITY (IN VITRO STUDIES)

Bacterial Source and Culture Conditions. Gram-negative (−ve) bacteria like *E. coli* (ATCC25922) and Gram-positive (+ve) bacteria like *Staphylococcus aureus* were the strains of bacteria that were employed. The culture medium employed was nutrient agar (g L^{-1}) pH = 7.3 ± 0.1. For 24−48 h, the plates were incubated at 37 °C. The paper disc assay method was used to determine antibacterial activity against the aforementioned pathogens.[20] A 0.6 mm-diameter disc of Whatman no. 1 filter paper was autoclaved for 20 min at 121 °C to sterilize it. Various chemicals (50 mg mL) were impregnated into the sterile discs. Surface inoculations from the broth culture of the tested microorganisms were made on evenly sized-agar plates. In each instance, the concentration was around 1.5 × 10^8 cfu mL^{-1}. The impregnated discs were placed on the medium, appropriately spaced apart, and plates were incubated at 37 °C for 24−48 h.[21] Thirty mg of chloramphenicol per disc was utilized. The attempted drugs' growth inhibition halos' diameter was measured and reported in millimeters. Three duplicate experiments were performed. The millimeters were used to measure the inhibitory zones, and Table 5 presents the data.

Structure−Activity Correlation. New 11 compounds **2**−**7** and **9**−**13**, were selected and evaluated in vitro for antibacterial activity against the bacterial strains *E. coli* and *Staphylococcus aureus*. Compounds **5**, **11**, **12**, and **13** are the most active derivatives when compared to the standard Chloramphenicol as a control. Obviously, the greater inhibition of these compounds may be due to the presence of the ester group in compounds **5** and **12**, in addition to the pyrimidine ring in the derivatives **11**, **12**, and **13** which have the enolic OH group. Also, compound **8** showed a good inhibition effect, which may be attributed to the presence of benzene sulphonyl moiety. The remaining compounds gave slightly lower reactivity than the previously mentioned compounds.

EXPERIMENTAL SECTION

General. Purchased from Across Organics, all reagents and solvents were utilized without additional purification. IR (Shimadzu 408 spectrometer utilizing KBr pellet technique) and mass spectrometry were used to characterize each new chemical (HP Model, MS 5988 and AmD 402/3, El 70 ev), in addition to ^{1}H NMR 200, 300 MHz chemical shifts are relative to TMS as an internal reference. Elemental analysis and mass spectra were carried out at the "Micro Analytical Center" of Cairo University. Starting material: *cis*-1,2,3,6-tetrahydrophthalic anhydride 98% mp 99−102 °C (Merck, 8.00742.1000).

The antimicrobial evaluation was carried out at "The Central Laboratory" of South Valley University.

General Procedure for Preparation of the Imides 2−7. A mixture of 1,2,3,6-tetrahydrophthalic anhydride (**1**) (0.3 g, 2 mmol) and appropriate amines, namely, benzylamine, *o*-aminothiophenol, *p*-aminoacetophenone, *p*-aminoethylbenzoate, ethanolamine and glycine (2 mmol) in glacial acetic acid (10 mL) was refluxed for (2−3 h). After cooling, the solid forms were filtered off and crystallized from ethanol to give the 2-aryl-3a,4,7,7a-tetrahydroisoindol-1,3-diones **2**−**7** (cf. Tables 1 and 2, Scheme 1).

2-Phenylsulphonyloxy-3a,4,7,7atetrahydroisoindol-1,3-dione (8). 2-phenylsulphonyloxy-3a,4,7,7a-tetrahydroisoindol-1,3-dione (**8**) was prepared from 1,2,3,6-tetrahydrophthalic anhydride (**1**) according to the method mentioned in Aly et al. and Abo-Bakr et al.[14,15]

General Procedure for the Preparation of Tetrahydroquinazoline 9−13. 2-phenylsulphonyloxy-3a,4,7,7a-tetrahydroisoindol-1,3-dione (**8**) (0.5 g, 1 mmol) was refluxed with cyclohexylamine, butylamine, benzylamine, *p*-aminoacetophenone, *p*-aminoethylbenzoate (0.1 g, 2 mmol) in glacial acetic acid or dry toluene for 3 h. After cooling, the precipitate formed was washed well with benzene and crystallized from toluene to give *N*-alkyl-1,2,3,6-tetrahydroquinazoline-2,4-dione **9**−**13** (cf. Tables 1 and 2, Scheme 3).

https://doi.org/10.1021/acsomega.4c01176
ACS Omega 2024, 9, 18566−18575

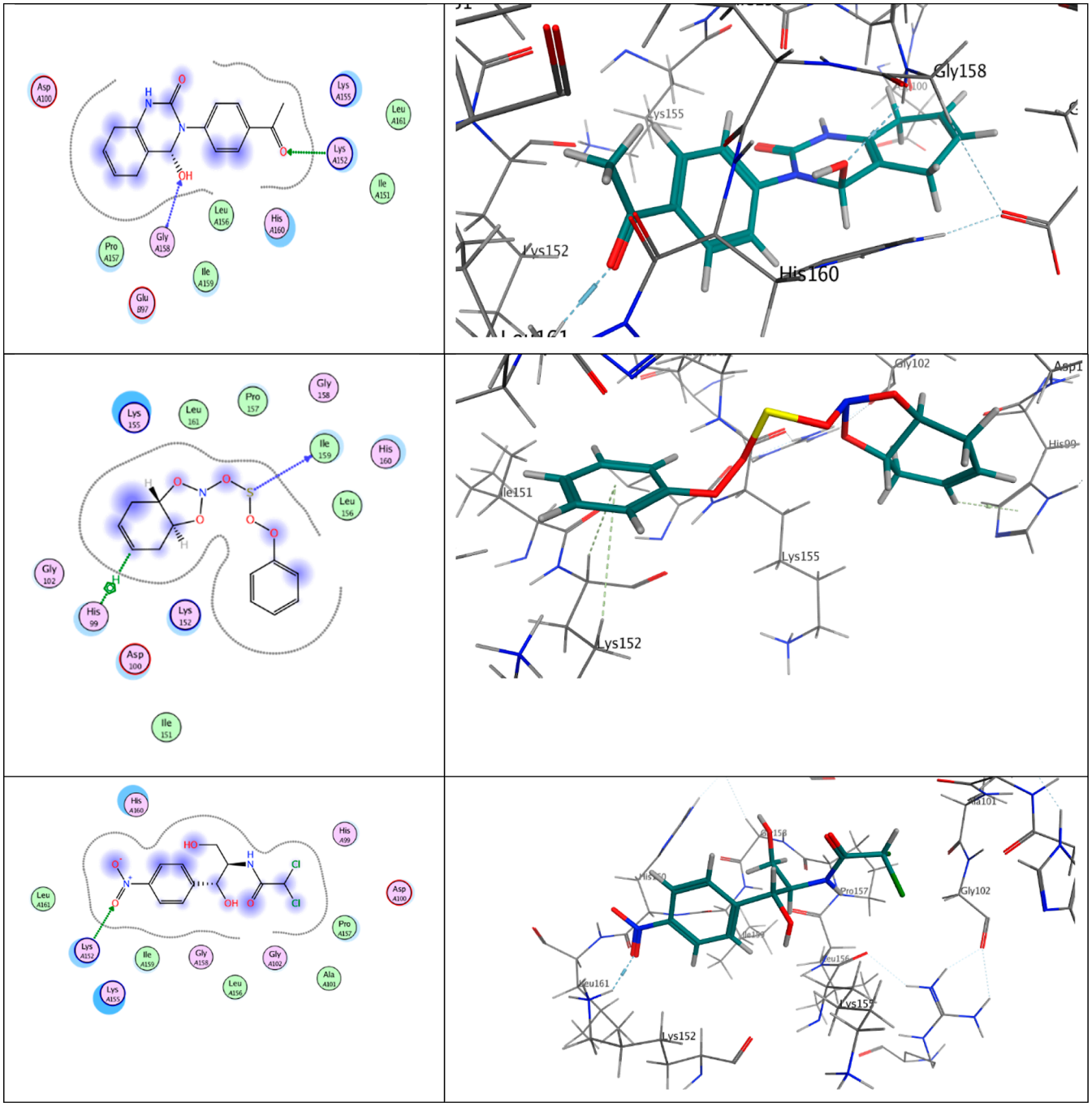

Figure 3. 2D (left side) and 3D (right side) docking orientations of the best-docked compounds **8**, **13**, and positive control with the active site pocket of PBP3.

Molecular Docking Approach. An in silico analysis was carried out by using **MOE 2014.09**[22] to assess the affinity and orientation of the freshly synthesized compounds against the active site of the target proteins PBP2a (PDB ID: 5m18) and PBP3 (4bjq). The X-ray crystal structure was provided with very good resolutions 1.98 and 2.10 Å, respectively.[23] The tested drugs were sketched using PubChem (https://pubchem.ncbi.nlm.nih.gov/). After importing them into MOE, all the problems with the protein structures were fixed using the program's structure preparation wizard. After all solvent molecules were removed from the structures and hydrogen atoms in their usual geometry were added, the structures, targeted protein, and tested compounds were then subjected to energy minimization using Amber12 as a force field. Both prepared crystal structure proteins and compounds were saved in the form of an MDB file to be fit in occurring molecular docking calculations.[24] The resulting poses were examined once the docking operations were finished, and the best ones with the best binding energy scores and acceptable rmsd_refine values were chosen.[25] Additionally, a program validation procedure was initially carried out and supported by a low rmsd value.

The cocrystallized ligand was positioned at the target's active site for analysis. to confirm the accuracy of the docking process. The rmsd value was calculated, and it was found to be

https://doi.org/10.1021/acsomega.4c01176
ACS Omega 2024, 9, 18566−18575

Table 5. Impact of the Manufactured Compounds on the Growth of Bacteria[a]

sample	bacterial growth inhibition zone diameter (mm)	
	Gram (−ve) bacteria E. coli	Gram (+ve) bacteria Staphylococcus aureus
2	21 ± 0.7	22 ± 0.5
3	19 ± 0.4	18 ± 0.3
4	17 ± 0.3	16 ± 0.5
5	22 ± 0.5	19 ± 0.7
6	15 ± 0.3	17 ± 0.4
7	23 ± 0.2	20 ± 0.3
8	24 ± 0.5	23 ± 0.5
9	20 ± 0.6	22 ± 0.2
10	21 ± 0.5	20 ± 0.8
11	24 ± 0.2	21 ± 0.6
12	22 ± 0.4	26 ± 0.6
13	27 ± 0.4	25 ± 0.3
chloro-amphenicol (30 mg)	30	30

[a]±: Plus or minus the corresponding value.

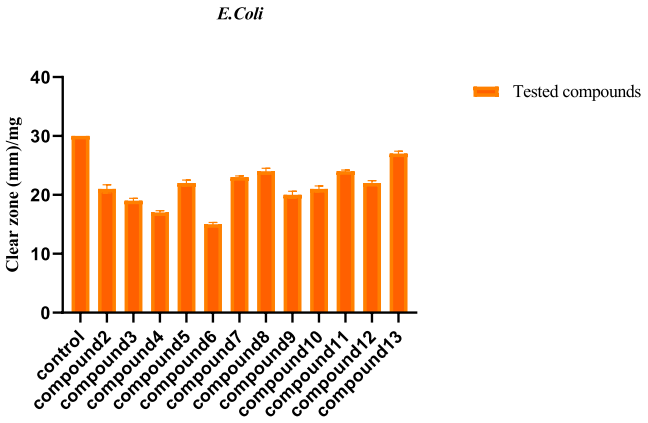

Figure 4. Electrostatic potential maps of the ligands.

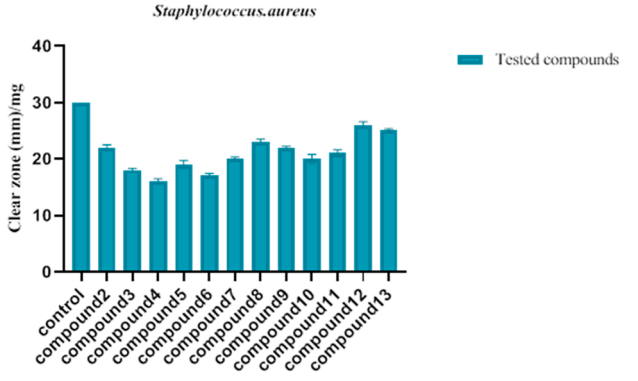

Figure 5. Electrostatic potential maps of the ligands.

less than 2, indicating the suitability of the docking methodology.[26]

CONCLUSIONS

In general, we used a convenient synthetic approach to the new six imides **2**−**7** based on the key precursor 1,2,3,6-tetrahydrophthalic anhydride (**1**) and the new five tetrahydroquinazoline derivatives **9**−**13** based on 2-phenylsulphonyloxy-3a,4,7,7a-tetrahydroisoindol-1,3-dione (**8**). The IR, ^{1}H NMR, MS, and elemental analyses confirmed their chemical structures. A total of newly synthesized heterocyclic-containing nitrogen compounds were subjected to protocol docking against PBP3, and PBP2a of staphylococcus and *E. coli*, respectively. The tested compounds exhibited variable binding energy scores toward *Staphylococcus* and *E. coli*. due to the various binding interactions, confirmed that these compounds could be sealed in both the PBP3 and PBP2a proteins' active site pockets of *E. coli* and *Staphylococcus* by attaching to amino acid residue in a suitable pose. Among these compounds, we highlighted the compounds that were found to exhibit the most acceptable rmsd_refine values and the best binding scores **12** and **5**, and **13** and **8** against PBP2a and PBP3, respectively. So, these highlighted compounds are promising and could be used as a therapeutic antibacterial agent after emphasizing the results via in vitro biological activity.

ASSOCIATED CONTENT

Supporting Information

The Supporting Information is available free of charge at https://pubs.acs.org/doi/10.1021/acsomega.4c01176.

(PDF)

AUTHOR INFORMATION

Corresponding Authors

Eman Fayad − *Department of Biotechnology, College of Sciences, Taif University, Taif 21944, Saudi Arabia*; orcid.org/0000-0003-2916-0254; Email: hhhh_fayed@yahoo.co.uk

Ahmed M. Abo-Bakr − *Chemistry Department, Faculty of Science, South Valley University, Qena 83523, Egypt*; Email: ahmadbaker672@sci.svu.edu.eg

Authors

Dalal Nasser Binjawhar − *Department of Chemistry, College of Science, Princess Nourah Bint Abdulrahman University, Riyadh 11671, Saudi Arabia*

Ola A. Abu Ali − *Department of Chemistry, College of Science, Taif University, Taif 21944, Saudi Arabia*

Arwa Sultan Alqahtani − *Department of Chemistry, College of Science, Imam Mohammad Ibn Saud Islamic University (IMSIU), Riyadh 11623, Saudi Arabia*

Antonous. M. Mekhael − *Cotton Leaf Worm Department, Plant Protection Research Institute, Agriculture Research Center, Giza 12611, Egypt*

Fayza M. Sadek − *Radiation Sciences Department, Medical Research Institution, Alexandria University, Alexandria 5424041, Egypt*

Complete contact information is available at: https://pubs.acs.org/10.1021/acsomega.4c01176

Notes

The authors declare no competing financial interest.

ACKNOWLEDGMENTS

The authors extend their appreciation to Princess Nourah bint Abdulrahman University Researchers Supporting Project number (PNURSP2024R155) Princess Nourah bint Abdulrahman University, Riyadh, Saudi Arabia.

REFERENCES

(1) Jafari, E.; Hassanzadeh, F. Cyclic imide derivatives: As promising scaffold for the synthesis of antimicrobial agents. *J. Res. Med. Sci.* **2018**, *23* (1), 53.

(2) Davood, A.; Iman, M.; Pouriaiee, H.; Shafaroodi, H.; Akhbari, S.; Azimidoost, L.; Rahmatpour, S. Novel derivatives of phthalimide with potent anticonvulsant activity in PTZ and MES seizure models. *Iran. J. Basic Med. Sci.* **2017**, *20* (4), 430−437.

(3) Filho, V. C.; Corrêa, R.; Vaz, Z.; Calixto, J. B.; Nunes, R. J.; Pinheiro, T. R.; Andricopulo, A. D.; Yunes, R. A. Further studies on analgesic activity of cyclic imides. *Il Farmaco* **1998**, *53* (1), 55−57.

(4) Kumar, A.; Banerjee, S.; Roy, P.; Sondhi, S. M.; Sharma, A. Solvent free, catalyst free, microwave or grinding assisted synthesis of bis-cyclic imide derivatives and their evaluation for anticancer activity. *Bioorg. Med. Chem. Lett.* **2017**, *27* (3), 501−504.

(5) Havera, H. J. Derivatives of 1,3-disubstituted 2,4(1H,3H)-quinazolinediones as possible peripheral vasodilators or antihypertensive agents. *J. Med. Chem.* **1979**, *22* (12), 1548−1550.

(6) Chatturong, U.; Chootip, K.; Martin, H.; Tournier-Nappey, M.; Ingkaninan, K.; Temkitthawon, P.; Sermsenaphorn, S.; Somarin, T.; Konsue, A.; Gleeson, M. P.; et al. The new quinazoline derivative (N-methyl-N-[(thiophen-2-yl)methyl]quinazoline-2,4-diamine) vasodilates isolated mesenteric arteries through endothelium-independent mechanisms and has acute hypotensive effects in Wistar rats. *Eur. J. Pharmacol.* **2023**, *953* (175829), 175829.

(7) Ghodge, B.; Kshirsagar, A.; Navghare, V. Synthesis, characterization, and investigation of the anti-inflammatory effect of 2,3-disubstituted quinazoline-4(1H)-one. *Beni-Suef Univ. J. Basic App. Sci.* **2020**, *9* (1), 30.

(8) Jafari, E.; Khajouei, M. R.; Hassanzadeh, F.; Hakimelahi, G. H.; Khodarahmi, G. A. Quinazolinone and quinazoline derivatives: recent structures with potent antimicrobial and cytotoxic activities. *Res. Pharm. Sci.* **2016**, *11* (1), 1−14.

(9) Ventola, C. L. The antibiotic resistance crisis: part 1: causes and threats. *Pharm. Ther.* **2015**, *40* (4), 277−283.

(10) Uddin, T. M.; Chakraborty, A. J.; Khusro, A.; Zidan, B. R. M.; Mitra, S.; Emran, T. B.; Dhama, K.; Ripon, M. K. H.; Gajdács, M.; Sahibzada, M. U. K.; et al. Antibiotic resistance in microbes: History, mechanisms, therapeutic strategies and future prospects. *J. Infect. Public Health* **2021**, *14* (12), 1750−1766.

(11) Zapun, A.; Contreras-Martel, C.; Vernet, T. Penicillin-binding proteins and β-lactam resistance. *FEMS Microbiol. Rev.* **2008**, *32* (2), 361−385.

(12) Talip Al-mohanna, M. *Morphology and Classification of Bacteria Growth and Laboratory Maintenance of Vibrio cholerae View Project Detction the Alpha Hemolysin Genes of E. coli by PCR View Project 2016*, 2016. https://www.researchgate.net/publication/315803754.

(13) Bernáth, G.; Stájer, G.; Szabó, A. E.; Fölöp, F.; Sohár, P. Stereochemical studies 83 saturated heterocycles 76. *Tetrahedron* **1985**, *41* (7), 1353−1365.

(14) Fahmy, A. F. M.; Aly, N. F.; Orabi, M. O. Phthalimides. III. Ammonolysis, Aminolysis, Hydrazinolysis, Pyrolysis, and Action of Grignard Reagents on Phthalimide Derivatives. *Bull. Chem. Soc. Jpn.* **1978**, *51* (7), 2148−2152.

(15) Abo-Bakr, A.; Taha, M.; Mekhael, A.; Mohamed, M. New Cyclic Imides and Quinazolin-2,4-diones Based on 1,2,3,6-Tetrahydrophthalic anhydride: Synthesis, Semiempirical Study and in vitro Evaluation. *Egypt. J. Chem.* **2022**, *0* (0), 0.

(16) Mason, J. T. Mixing behavior of symmetric chain length and mixed chain length phosphatidylcholines in two-component multilamellar bilayers: evidence for gel and liquid-crystalline phase immiscibility. *Biochemistry* **1988**, *27* (12), 4421−4429.

(17) Naaz, F.; Srivastava, R.; Singh, A.; Singh, N.; Verma, R.; Singh, V. K.; Singh, R. K. Molecular modeling, synthesis, antibacterial and cytotoxicity evaluation of sulfonamide derivatives of benzimidazole, indazole, benzothiazole and thiazole. *Bioorg. Med. Chem.* **2018**, *26* (12), 3414−3428.

(18) Alotaibi, S. H.; Amer, H. H. Synthesis, spectroscopic and molecular docking studies on new schiff bases, nucleosides and α-aminophosphonate derivatives as antibacterial agents. *Saudi J. Biol. Sci.* **2020**, *27* (12), 3481−3488.

(19) Mahasenan, K. V.; Molina, R.; Bouley, R.; Batuecas, M. T.; Fisher, J. F.; Hermoso, J. A.; Chang, M.; Mobashery, S. Conformational dynamics in penicillin-binding protein 2a of methicillin-resistant staphylococcus aureus, allosteric communication network and enablement of catalysis. *J. Am. Chem. Soc.* **2017**, *139* (5), 2102−2110.

(20) Balouiri, M.; Sadiki, M.; Ibnsouda, S. K. Methods for in vitro evaluating antimicrobial activity: A review. *J. Pharm. Anal.* **2016**, *6* (2), 71−79.

(21) Haghjoo, B.; Lee, L. H.; Habiba, U.; Tahir, H.; Olabi, M.; Chu, T.-C. The synergistic effects of green tea polyphenols and antibiotics against potential pathogens. *Adv. Biosci. Biotechnol.* **2013**, *04* (11), 959−967.

(22) Vilar, S.; Cozza, G.; Moro, S. Medicinal chemistry and the molecular operating environment (MOE): Application of QSAR and molecular docking to drug discovery. *Curr. Top. Med. Chem.* **2008**, *8* (18), 1555−1572.

(23) Dubach, V. R. A.; Guskov, A. The resolution in X-ray crystallography and single-particle cryogenic electron microscopy. *Crystals* **2020**, *10* (7), 580.

(24) Al-Karmalawy, A. A.; Dahab, M. A.; Metwaly, A. M.; Elhady, S. S.; Elkaeed, E. B.; Eissa, I. H.; Darwish, K. M. Molecular docking and dynamics simulation revealed the potential inhibitory activity of ACEIs against SARS-CoV-2 targeting the hACE2 receptor. *Front. Chem.* **2021**, *9*, 661230.

(25) Meli, R.; Morris, G. M.; Biggin, P. C. Scoring functions for protein-ligand binding affinity prediction using structure-based deep learning: A review. *Front. Bioinform.* **2022**, *2*, 2.

(26) Kontoyianni, M.; McClellan, L. M.; Sokol, G. S. Evaluation of docking performance: comparative data on docking algorithms. *J. Med. Chem.* **2004**, *47* (3), 558−565.

https://doi.org/10.1021/acsomega.4c01176
ACS Omega 2024, 9, 18566−18575